SO2+(C–X) fluorescence from Penning ionization of SO2

ARTICLE *in* INTERNATIONAL JOURNAL OF MASS SPECTROMETRY AND ION PHYSICS · NOVEMBER 1978

DOI: 10.1016/0020-7381(78)80090-4

4 AUTHORS, INCLUDING:

Masaharu Tsuji
Kyushu University
441 PUBLICATIONS **6,229** CITATIONS

SEE PROFILE

International Journal of Mass Spectrometry and Ion Physics, 28 (1978) 257—265

$SO_2^+(\tilde{C} - \tilde{X})$ FLUORESCENCE FROM PENNING IONIZATION OF SO_2

M. TSUJI, H. FUKUTOME, K. TSUJI and Y. NISHIMURA

Research Institute of Industrial Science 86, Kyushu University, Hakozaki, Fukuoka 812 (Japan)

(First received 10 January 1978; in final form 20 February 1978)

ABSTRACT

In addition to $SO(A^3\Pi - X^3\Sigma^-)$ and $SO_2(\tilde{A}^1B_1 - \tilde{X}^1A_1)$ emission, the $\tilde{C}^2B_2(v_1', 0, 0) - \tilde{X}^2A_1(v_1'', 0, 0)$ transition of SO_2^+ fluorescence, which has its origin at 3376 ± 2 Å, has been identified in the reaction of $He(2^3S)$ with SO_2. The symmetrical stretching vibrational frequencies of the $\tilde{X}$ and $\tilde{C}$ states of SO_2^+ have been determined to be 1259 ± 13 and 788 ± 14 cm^{-1}.

INTRODUCTION

The electronically and vibrationally excited states of sulfur dioxide cation have been investigated by photoelectron spectrometry and optical emission spectrometry. Eland and Danby [1], and Turner et al. [2] have reported the high-resolution HeI photoelectron spectra of SO_2. Lloyd and Roberts [3] have analyzed the HeI and HeII photoelectron spectra above 17 eV. Eland et al. [4] have attempted to observe SO_2^+ emission excited by the HeI line. Although they have detected no emission, the fluorescence quantum yield of $SO_2^+(\tilde{C} + \tilde{D})$ has been estimated to be larger than $2.3 \pm 1.7 \times 10^{-4}$ by the photon—photoion coincidence method. Recently Wu and Yencha [5] have observed a strong, extensive emission band system from 300 to 550 nm in the $He(2^3S) + SO_2$ reaction and assigned it to the $\tilde{B}^2A_1 - \tilde{X}^2A_1$ transition of SO_2^+. We have re-examined the emission spectrum of SO_2 in a helium afterglow from 200 to 510 nm at a medium resolution. Our measurements were more sensitive than those of Wu and Yencha, enabling a more precise analysis of the complicated spectrum observed to be carried out. In comparison with the high-resolution photoelectron spectra, a new reasonable assignment for the $SO_2^+(\tilde{C}^2B_2 - \tilde{X}^2A_1)$ emission has been found [6].

EXPERIMENTAL

The flowing afterglow apparatus used is shown in Fig. 1. The quartz flow tube (12 mm in diameter) and the Pyrex reaction cell (35 mm in diameter) were evacuated continuously by a 7000 l min^{-1} oil rotary pump. Before

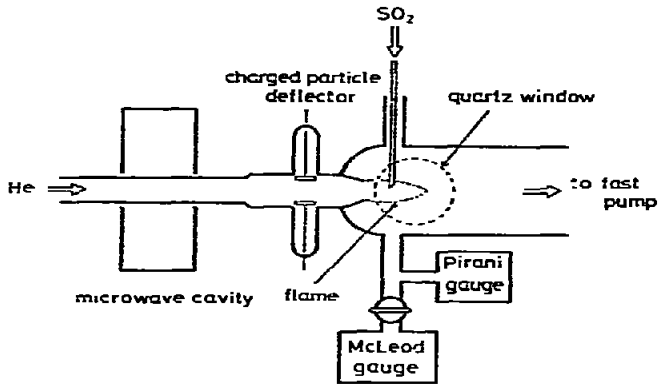

Fig. 1. Schematic diagram of the flowing afterglow apparatus.

entering the discharge section, helium gas (>99.99% purity) was purified by passage through a liquid nitrogen trap packed with activated molecular sieve (Wako Pure Chemical Ind. type 5A 1/16). The metastable He(2^3S) atoms were generated by a 2450-MHz microwave discharge in the quartz tube with the input power at 80 W. The effect of charged particles probably involved in the discharge flow was examined by applying an electrostatic potential to a charged particle deflector. Sulfur dioxide (>99.9% purity) and oxygen (>99.99% purity) were used without further purification. The sample gas was introduced through a stainless steel nozzle 0.4 mm in diameter at about 15 cm downstream from the discharge section. The gas pressure was measured by a Pirani gauge (ULVAC GP-2T) calibrated against a McLeod gauge. The helium pressure was 1—2 torr and the sample gas pressure was 5×10^{-3} -5×10^{-2} torr.

The reaction flame was focused by quartz lenses on the inlet slit of a scanning monochromator (Shimadzu GE-100) with a 1200 line mm^{-1} grating blazed at 300 nm; its reciprocal dispersion was 8.3 Å mm^{-1}. The photons were detected photoelectrically with a photomultiplier (Hamamatsu TV R106UH) and an OP amplifier (Burr—Brown 3523J). The wavelength was calibrated by means of a low-pressure mercury lamp (Hamamatsu TV L987-03); its error was estimated to be within ±2 Å. The vibrational analysis of the observed spectrum was carried out by use of wavelength with maximum intensity.

RESULTS AND DISCUSSION

Figure 2 shows a typical emission spectrum of SO_2 from 240 to 460 nm in a helium afterglow. Above weak continuous features extending from 265 to 440 nm, numerous discrete bands can be observed. Possible active species responsible for the appearance of these photoemission are He(2^3S), He(2^1S),

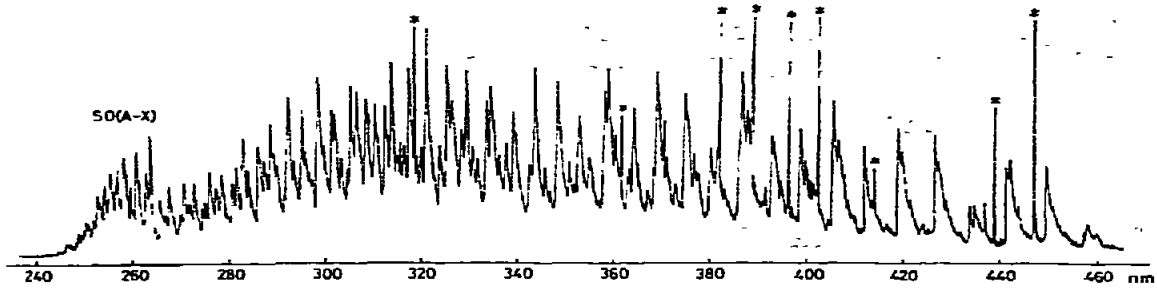

Fig. 2. A typical emission spectrum of SO_2 in a helium afterglow. Lines marked * are stray HeI lines.

He^+, and electrons in the helium afterglow at 1—2 torr. The contribution from He^+ and electrons is negligible, because the intensities of the observed spectra did not show any appreciable change, when a d.c. voltage of 0—100 V was applied to the deflector electrodes. It is known that metastable $He(2^1S)$ atoms rapidly convert to $He(2^3S)$ by elastic collisions with electrons [7]. Therefore, the predominant energy carrier under experimental conditions here are metastable $He(2^3S)$ atoms with enough energy (19.8 eV) to ionize and dissociate sulfur dioxide. The energy-level diagrams of various possible products in the $He(2^3S) + SO_2$ reaction are shown in Fig. 3. Although Wu and Yencha [5] have reported the detection of weak $SO(B^3\Sigma^- - X^3\Sigma^-)$ emission, this band system could not be identified in our spectrum. Instead of the B—X system, the $A^3\Pi - X^3\Sigma^-$ transition of SO, which was absent in their spectrum, was observed here in the 240—265-nm region.

The fluorescence and phosphorescence spectra of SO_2 have been studied extensively by UV photo-excitation. Mettee [14] has reported that the fluorescence spectrum of SO_2 became diffuse with an increase in the excitation energy, and at excitation by the 265-nm line, a discrete resonance band was no longer observed. Wu and Yencha [5] have reported the observation of $SO_2(\tilde{A}^1B_1 - \tilde{X}^1A_1)$ emission in the $He(2^3S) + SO_2$ system. However, their spectrum does not show what kind of SO_2 fluorescence, discrete band and/or continuous band, was identified. Although the discrete band which was observed by Mettee [14] at low excitation energies is not identified in our spectrum, the underlying continuous emission was assigned to the $\tilde{A}^1B_1 - \tilde{X}^1A_1$ transition of SO_2, because its observed spectral range is in good agreement with his fluorescence spectrum at the highest excitation energy. The absence of structure indicates that the excitation into lower vibrational levels of the $\tilde{A}^1B_1$ state is of little importance in the $He(2^3S) + SO_2$ reaction. Since the formation of excited parent species in a helium afterglow has not been reported, the present finding of the photoemission from the singlet parent species is noteworthy.

The expanded emission spectrum in the 310—510-nm region is shown in

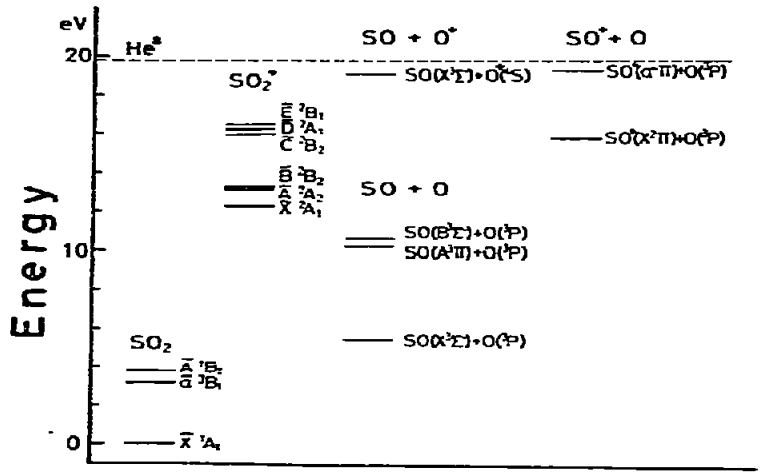

Fig. 3. The energy-level diagrams of possible products in the $He(2^3S) + SO_2$ reaction. The diagrams were obtained by use of the excitation energies of SO_2 [8] and SO [9], the ionization energies of SO_2 [1,3], O [10], and SO [11], and the dissociation energy of $D(OS—O) = 5.5$ eV [12]. SO_2^+ was assigned by reference with the analyses of Hillier and Saunders [13] and of Lloyd and Roberts [3].

Fig. 4. The most striking feature of the SO_2 spectrum in the reaction with $He(2^3S)$ is the appearance of a rather strong, extensive band system, which has not been observed by the impact of VUV photons [4], 75—350-eV electrons [15], and 2—3-keV_{lab} Ar^+ ions [16]. On the basis of the data in Fig. 3, energetically possible candidates for this emission are SO^+ (a — X) and $SO_2^+(\tilde{C}, \tilde{D}, \tilde{E} — \tilde{X}$ and $\tilde{C}, \tilde{D}, \tilde{E} — \tilde{A})$. The transition energies between various vibrational levels can be estimated by the high-resolution photoelectron data of SO [11] and SO_2 [1—3]. We have calculated the transition energies of the two components of SO^+, $a^4\Pi — X^2\Pi_{1/2,3/2}$, assuming the vibrational intervals of the $X^2\Pi$ and $a^4\Pi$ states to be about 1360 and 800 cm^{-1}. Although an emission series was identified in agreement with the calculated transition energies, irregular variations were found in the intensity distribution of the two components. For the further clarification of the presence of the SO^+ (a—X) emission, the emission spectrum of O_2 was measured under identical experimental conditions, because analogous ionic states exist in molecular oxygen [11]. The observed spectrum for the $He(2^3S) + O_2$ reaction was very similar to that of Richardson and Setser [17]. The predominant emission was the $A^2\Pi_u — X^2\Pi_g$ system of O_2^+. The spin-forbidden transition $a^4\Pi — X^2\Pi$ was not identified in the spectral range expected from the photoelectron data. These results indicate that SO^+ (a — X) emission from SO_2 is excluded from the possible candidates.

Remaining possible emissive species is SO_2^+ for which six states are known by photoelectron spectroscopy [1—3]: $\tilde{X}$ (adiabatic $IP = 12.3$ eV), $\tilde{A}$ (13.0

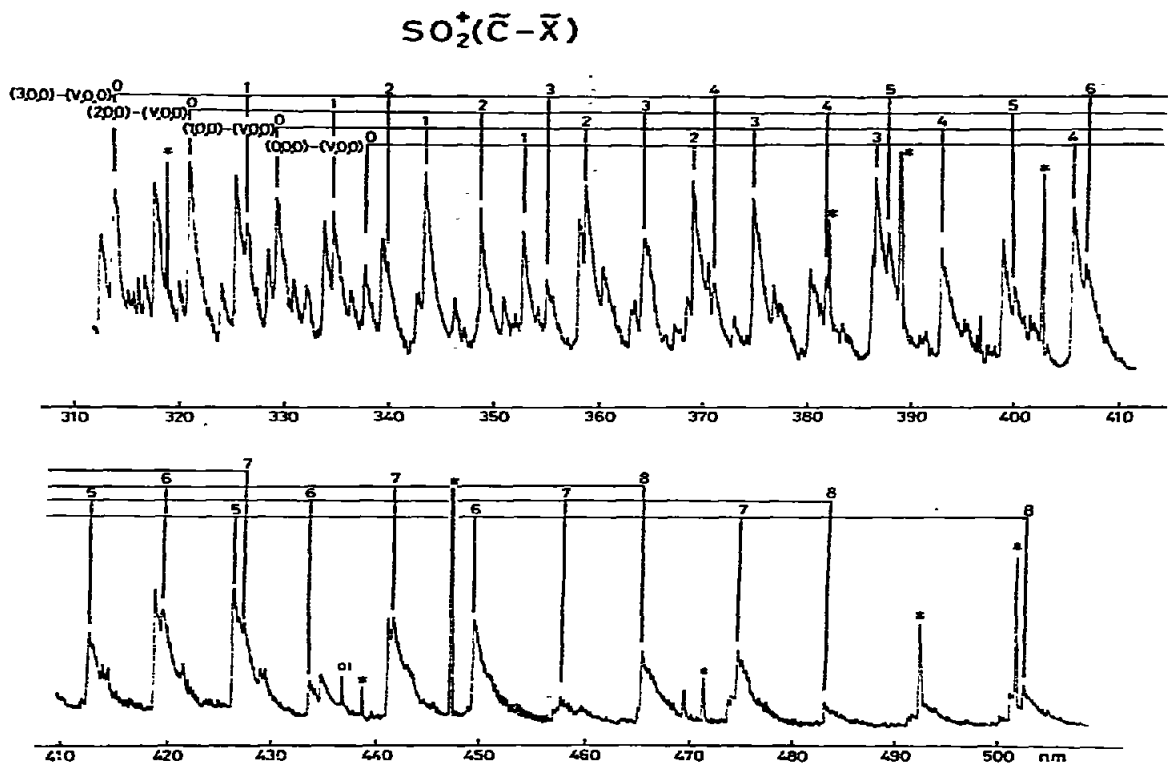

Fig. 4. Fluorescence spectrum of the $SO_2^+[\tilde{C}^2B_2(v_1', 0, 0)-\tilde{X}^2A_1(v_1'', 0, 0)]$ system produced by the He(2^3S) Penning ionization of SO_2. Lines marked * are stray HeI lines.

eV), $\tilde{B}$ (13.2 eV), $\tilde{C}$ (16.0 eV), $\tilde{D}$ (16.3 eV), and $\tilde{E}$ (16.5 eV). The ground ionic state arises from the removal of an electron from the sulfur lone-pair $8a_1$ orbital, whereas the $\tilde{A}$, $\tilde{B}$, $\tilde{C}$, and $\tilde{D}$ states result from the loss of an electron from the $1a_2$, $5b_2$, $2b_1$, and $7a_1$ orbitals, respectively [13]. At first, we attempted to interpret the observed spectrum according to Wu and Yencha's analysis of $SO_2^+(\tilde{C}-\tilde{X})$ [5]. The corresponding band system of $SO_2^+(\tilde{C}-\tilde{X})$ was found in our spectrum, therefore, a similar Delandres table was obtained. However, the following serious defects, as is also found in their table, came out. (1) There are large differences between the observed wave-number of the band origin (29965 ± 15 cm^{-1}) and the estimated values from the photoelectron data (29730 ± 121 [1] and 29682 ± 161 [2] cm^{-1}). (2) The transition energies of the (0, 0, 0) — (v_1'', 0, 0) bands for $0 \leqslant v_1'' \leqslant 3$ are systematically about 100 cm^{-1} lower than those estimated from the other bands, namely, the vibrational interval derived from the difference between the (0, 0, 0) — (3, 0, 0) and (0, 0, 0) — (4, 0, 0) bands is about 100 cm^{-1} smaller than the other intervals.

TABLE I

Delandres table for the $\tilde{C}^2B_2(v_1',0,0) - \tilde{X}^2A_1(v_1'',0,0)$ transition of SO_2^+

v_1'	v_1'' (cm^{-1})								
	0	1	2	3	4	5	6	7	8
0	29620 (1263)	28357 (1246)	27111 (1236)	25875 (1217)	24658 (1210)	23448 (1191)	22257 (1187)	21070 (1166)	19904
	(770)	(775)	(776)	(813)	(800)	(784)	(800)	(779)	(791)
1	30390 (1258)	29132 (1245)	27887 (1199)	26688 (1230)	25458 (1226)	24232 (1175)	23057 (1208)	21849 (1154)	20695
	(784)	(768)	(802)	(766)	(739)	(770)	(769)	(794)	(792)
2	31174 (1274)	29900 (1211)	28689 (1235)	27454 (1257)	26197 (1195)	25002 (1176)	23826 (1183)	22643 (1156)	21487
	(717)	(749)	(744)	(721)	(736)	(791)	(764)	(749)	
3	31891 (1242)	30649 (1216)	29433 (1258)	28175 (1212)	26963 (1170)	25793 (1203)	24590 (1198)	23392	

Taking into account the discrepancy between the observed origin and the estimated values from photoelectron data, a second attempt was made to analyze the observed spectrum. This time we found the calculated wavelengths to fit the observed spectrum very well, when the value of 3376 ± 2 Å was assigned to the band origin. The detailed vibrational assignment is given in Fig. 3. As shown in Fig. 3, most of the prominent discrete bands in the 310—510-nm region are ascribable to the $\tilde{C}^2B_2 - \tilde{X}^2A_1$ transition of SO_2^+, where the upper and lower states are represented according to the assignment of Lloyd and Roberts [3]. In the observed spectral range, $\tilde{C}^2B_2(v_1', 0, 0) - \tilde{X}^2A_1(v_1'', 0, 0)$ for $0 \leqslant v_1'' \leqslant 8$ with $0 \leqslant v_1' \leqslant 3$ can be identified. The Delandres table for the $\tilde{C}^2B_2 - \tilde{X}^2A_1$ transition of SO_2^+ is given in Table 1. The observed band origin of 29620 ± 18 cm^{-1} agrees reasonably well with the calculated values of 29730 ± 121 [1] and 29682 ± 161 [2] cm^{-1} from photoelectron data. Combining the emission photon energies with the ionization potential of the $\tilde{X}^2A_1(0, 0, 0)$ level, which is reported to be 12.305 eV [1], the ionization potentials for the vibrational levels of the $\tilde{X}^2A_1$ and $\tilde{C}^2B_2$ states are obtained and listed in Table 2.

One of the most prominent features in the emission spectrum of SO_2

TABLE 2

The ionization potentials for the $\tilde{X}^2A_1$ and $\tilde{C}^2B_2$ vibrational levels obtained from the emission spectrum. Photoelectron data are also given for comparison

Vibrational levels	Ionization potentials (eV)			
	Emission spectrum Present work	Photoelectron spectra		
		Eland and Danby *	Lloyd and Roberts **	Turner et al. ***
$\tilde{X}^2A_1$				
(0,0,0)	12.305	12.305		12.29(0)
(1,0,0)	12.461(2) ⋆			
(2,0,0)	12.613(2)			
(3,0,0)	12.766(3)			
(4,0,0)	12.919(2)			
(5,0,0)	13.067(3)			
(6,0,0)	13.214(2)			
(7,0,0)	13.353(1)			
(8,0,0)	13.506(1)			
$\tilde{C}^2B_2$				
(0,0,0)	15.977(2)	15.986	15.992(3)	15.97(2)
(1,0,0)	16.075(4)	16.092	16.090(3)	
(2,0,0)	16.171(5)	16.188	16.189(5)	
(3,0,0)	16.264(5)	16.284	16.286(6)	

* Ref. 1.
** Ref. 3.
*** Ref. 2.
⋆ Quantities in parentheses are standard deviations.

TABLE 3

The symmetrical stretching vibrational frequencies for the $\tilde{X}$ and $\tilde{C}$ states of SO_2^+

Electronic states	Vibrational frequencies (cm^{-1})			
	Emission spectrum Present work	Photoelectron spectra		
		Eland and Danby *	Lloyd and Roberts **	Turner et al. ***
Molecular ground state 1151 ^				
$\tilde{X}^2A_1$	1259 ± 13	—	—	—
$\tilde{C}^2B_2$	788 ± 14	816 ± 15	782 ± 20	850

* Ref. 1; ** ref. 3; *** ref. 2; ^ ref. 8.

by $He(2^3S)$ Penning ionization is an appearance of the progressions of the symmetrical stretching vibration in the ground state, which has not been observed in the photoelectron spectra. From an analysis of the $SO_2^+(\tilde{C} - \tilde{X})$ emission, the symmetrical stretching vibrational frequency of the ground ionic state was determined to be 1259 ± 13 cm^{-1}. Moreover, the symmetrical stretching vibrational frequency of the $\tilde{C}^2B_2$ state was determined to be 788 ± 14 cm^{-1}. This value is in good agreement with the photoelectron value of 782 ± 20 cm^{-1} [3], but it is slightly lower than other existing values of 816 ± 15 [1] and 850 [2] cm^{-1} as summarized in Table 3. An increase in the vibrational frequency of the ground ionic state compared with that of the molecular ground state shows an antibonding character for the sulfur lone-pair $8a_1$ orbital, while a large decrease in the vibrational frequency of the excited $\tilde{C}^2B_2$ state corresponds to the strongly bonding nature of the $2b_1$ orbital in S—O.

From the present optical study, it can be concluded that the major channel in the $He(2^3S) + SO_2$ reaction is the Penning ionization into the $\tilde{C}^2B_2$ state. Molecular excitation (SO_2^*) and dissociative excitation (SO^*) are minor reactions. The present observation of the SO_2^+ emission, which has not been detected by any other excitation techniques, lead us to conclude that Penning ionization is a promising way of generating ion fluorescence.

SUMMARY

The collisions of $He(2^3S)$ with SO_2 gave a relatively strong band system in the UV and visible regions, in addition to weaker emission from $SO(A - X)$ and $SO_2(\tilde{A} - \tilde{X})$. From the analysis on the basis of high-resolution photoelectron data, this band was assigned to the $\tilde{C}^2B_2(v_1', 0, 0) - \tilde{X}^2A_1(v_1'', 0, 0)$ transition of SO_2^+. The Delandres table for this transition and the ionization

potentials for the $\tilde{X}^2A_1(v_1'', 0, 0)$ and $\tilde{C}^2B_2(v_1', 0, 0)$ vibrational levels are given in Tables 1 and 2. The symmetrical stretching vibrational frequencies of the $\tilde{X}$ and $\tilde{C}$ states obtained from the analysis of the $SO_2^+(\tilde{C} - \tilde{X})$ fluorescence are summarized in Table 3.

ACKNOWLEDGEMENT

Financial aid by the Ministry of Education of Japan (Grant-in-Aid 274144) is acknowledged.

REFERENCES

1 J.H.D. Eland and C.J. Danby, Int. J. Mass Spectrom. Ion Phys., 1 (1968) 111.
2 D.W. Turner, C. Baker, A.D. Baker and C.R. Brundle, Molecular Photoelectron Spectroscopy, Wiley—Interscience, London, 1970.
3 D.R. Lloyd and P.J. Roberts, Mol. Phys., 26 (1973) 225.
4 J.H.D. Eland, M. Devoret and S. Leach, Chem. Phys. Lett., 43 (1976) 97.
5 K.T. Wu and A.J. Yencha, Can. J. Phys., 55 (1977) 767.
6 Readers should not be confused by the assignment of SO_2^+; Although Wu and Yencha [5] have assigned the ionic state with the adiabatic *IP* 16.0 eV to the $\tilde{B}$ state, we have ascribed it to the $\tilde{C}$ state.
7 A.V. Phelps, Phys. Rev., 99 (1955) 1307.
8 G. Herzberg, Electronic Spectra and Electronic Structure of Polyatomic Molecules, Van Nostrand Reinhold, New York, 1966.
9 R.W.B. Pearse and A.G. Gaydon, The Identification of Molecular Spectra, 4th edn., Chapman and Hall, London, 1976.
10 G. Herzberg, Atomic Spectra and Atomic Structure, Dover Publications, New York, 1944.
11 J.M. Dyke, L. Golob, N. Jonathan, A. Morris, M. Okuda and D.J. Smith, J. Chem. Soc., Faraday Trans. II, 70 (1974) 1818.
12 C. Lalo and C. Vermeil, J. Photochem., 3 (1974/75) 441.
13 I.H. Hillier and V.R. Saunders, Mol. Phys., 22 (1971) 193.
14 H.D. Mettee, J. Chem. Phys., 49 (1968) 1784.
15 W.H. Smith, J. Quant. Spectrosc. Radiat. Trans., 9 (1969) 1191; M. Tsuji, H. Fukutome, Y. Nishimura, T. Ogawa and N. Ishibashi, to be published.
16 H. Fukutome, M. Tsuji and Y. Nishimura, J. Phys. Soc. Jpn., 44 (1978) 1401.
17 W.C. Richardson and D.W. Setser, J. Chem. Phys., 58 (1973) 1809.